Integrable pair-transition-coupled nonlinear Schrödinger equations

Liming Ling[1] and Li-Chen Zhao[2,*]
[1]*School of Mathematics, South China University of Technology, 510640, Guangzhou, China*
[2]*Department of Physics, Northwest University, 710069, Xi'an, China*
(Received 20 February 2015; revised manuscript received 22 June 2015; published 25 August 2015)

We study integrable coupled nonlinear Schrödinger equations with pair particle transition between components. Based on exact solutions of the coupled model with attractive or repulsive interaction, we predict that some new dynamics of nonlinear excitations can exist, such as the striking transition dynamics of breathers, new excitation patterns for rogue waves, topological kink excitations, and other new stable excitation structures. In particular, we find that nonlinear wave solutions of this coupled system can be written as a linear superposition of solutions for the simplest scalar nonlinear Schrödinger equation. Possibilities to observe them are discussed in a cigar-shaped Bose-Einstein condensate with two hyperfine states. The results would enrich our knowledge on nonlinear excitations in many coupled nonlinear systems with transition coupling effects, such as multimode nonlinear fibers, coupled waveguides, and a multicomponent Bose-Einstein condensate system.

DOI: 10.1103/PhysRevE.92.022924 PACS number(s): 05.45.Yv, 02.30.Ik

I. INTRODUCTION

The integrable nonlinear model plays an exceptional role in the study of nonlinear wave dynamics [1]. It has been demonstrated that not only a fundamental state but also many nonlinear localized states can be stable in nonlinear system. Moreover, some fundamental physical mechanisms, e.g., modulation instability and Fermi-Pasta-Ulam recurrence, can be described well by an Akhmediev breather or other types of nonlinear waves. Many different integrable nonlinear equations have been presented and studied for different physical systems. Among them, the nonlinear Schrödinger equation (NLS) has been given much attention because of its widespread applications in optics, water wave tank, plasmas, and financial systems, as well as the quantum world of superfluids and Bose-Einstein condensates [2]. Recently, coupled NLSs (CNLS) have become a topic of intense research in theory, since the components are usually more than two practically for many physical systems [3–8]. Generally, the population or particle number in each component is conserved for integrable CNLSs. However, in practical physical systems, the particle numbers in each component are not necessarily conserved. For instance, in microscopic particle transport, the particle in one component can transfer to another component through quantum tunneling [9–15]. In such systems, particle population in each mode cannot be conserved, and dynamics of nonlinear waves are expected to be more exotic. But the CNLS with particle transition is usually nonintegrable [9], and it is not convenient to study for nonlinear wave dynamics analytically. Therefore, it is essential and meaningful to discover some integrable CNLS with particle transitions.

Recently two-mode CNLSs with pair-transition effects (CNLS-p) were shown to be integrable, for which the transition dynamics of some nonlinear waves can be investigated exactly based on the solutions [16]. Some types of nonlinear excitations for a similar integrable model have been obtained based on special Hirota bilinearization and the Darboux transformation (DT) [17], such as bright solitons [18] or rogue waves [19]. Based on the studies of CNLS without particle transition [3–8], we expect that there should be more abundant nonlinear excitations in the CNLS-p system.

In this paper, we revisit the CNLS-p derived from a Hamiltonian which can be used to describe dynamics of a one-dimensional two-component Bose-Einstein condensate system with particle transition. We present two different DT forms for the CNLS-p, which can be used to derive many different types of nonlinear localized wave solutions. In particular, these new types nonlinear wave solutions can be represented as the linear combination of well-known solutions for classical NLS. These solutions suggest that there are many new nonlinear excitations in the CNLS-p described systems, such as waterfall-like breathers, kink-dark solitons, rogue waves with particle transition dynamics, breather-soliton pairs, etc. Possibilities to observe them are discussed in a Bose condensate system.

II. THE COUPLED NONLINEAR SCHRÖDINGER EQUATIONS WITH PARTICLE TRANSITION

A one-dimensional two-component Bose-Einstein condensate system with particle transition can be described by the Hamiltonian $\hat{H} = \sum_j [\frac{\hbar^2}{2m}\partial_x^2 \hat{q}_j \hat{q}_j^\dagger + \frac{g_{j,j}}{2}\hat{n}_j\hat{n}_j + g_{j,3-j}\hat{n}_j\hat{n}_{3-j} + J_1(\hat{q}_j^\dagger \hat{q}_{3-j} + \hat{q}_{3-j}^\dagger \hat{q}_j) + \frac{J_2}{2}(\hat{q}_j^\dagger \hat{q}_j^\dagger \hat{q}_{3-j}\hat{q}_{3-j} + \hat{q}_{3-j}^\dagger \hat{q}_{3-j}^\dagger \hat{q}_j \hat{q}_j)]$ where $n_j = \hat{q}_j^\dagger \hat{q}_j$ is the particle number operator, and the symbol † represents the Hermite conjugation. $g_{i,i}$ and $g_{3-i,i}$ $(i = 1,2)$ are the internal and external interactions between atoms. J_1 and J_2 denote single particle and pair particle transition coupling strength separately [20,21]. In most studies, $J_{1,2}$ are set to be zero usually because it was believed that the presence of tunneling makes the systems become nonintegrable [5–8]. Recent experimental results in a double-well Bose-Einstein condensate suggested that pair tunneling can become dominant with strong interaction between atoms [22,23]. Therefore, we consider that the case for second-order transition is dominant, namely, $J_1 = 0$ and $J_2 \neq 0$. We find the integrable CNLS-p can be derived from the Hamiltonian with $g_{j,3-j} = 2g_{j,j} = 2J_2$.

It is convenient to set $g_{j,j} = -\sigma$ ($\sigma = \pm 1$ corresponds to attractive or repulsive interactions between atoms) without

*zhaolichen3@163.com

losing generality, for there is a trivial scalar transformation for different values. The corresponding dynamic evolution equation can be derived from the Heisenberg equation $\mathrm{i}\hbar(\partial\hat{q}_j/\partial t) = [\hat{q}_j, \hat{H}]$ for the field operator. Performing the mean field approximation $\langle\hat{q}_j\rangle = q_j$, we can get the following integrable CNLS-p with scale dimensions $m = \hbar = 1$:

$$\begin{aligned} &\mathrm{i}q_{1,t} + \tfrac{1}{2}q_{1,xx} + \sigma(|q_1|^2 + 2|q_2|^2)q_1 + \sigma q_2^2\bar{q}_1 = 0,\\ &\mathrm{i}q_{2,t} + \tfrac{1}{2}q_{2,xx} + \sigma(2|q_1|^2 + |q_2|^2)q_2 + \sigma q_1^2\bar{q}_2 = 0, \end{aligned} \tag{1}$$

where the symbol overbar represents the complex conjugation. The coupled model can be also used to describe the propagation of orthogonally polarized optical waves in an isotropic medium [24]. Bond soliton fiber laser and soliton interactions were studied in a similar coupled model [25,26]. The propagation of optical beams in terms of the two orthogonal modes of a planar waveguide where the beams are allowed to diffract only in one spatial dimension can be described by the coupled model with some constrains on the ratio of cross- and self-phase modulation coefficients, cross-phase modulation, and four-wave-mixing term [27,28]. What needs mentioning is that the above coupled equations without the last term usually are deemed as nonintegrable CNLSs [29]. However, when we add the particle transition term, the nonintegrable CNLSs become integrable, which was also proven by Painlevé analysis [17]. The bright soliton and rogue wave were studied for the model that the nonlinear coefficients and pair-transition coefficients are different [18,19].

III. THE LAX PAIR AND DARBOUX TRANSFORMATION

The integrable equations are found to admit the following Lax pair:

$$\begin{aligned} \Phi_x &= U(x,t;\lambda)\Phi,\\ \Phi_t &= V(x,t;\lambda)\Phi, \end{aligned} \tag{2}$$

where

$$\begin{aligned} U(x,t;\lambda) &\equiv \mathrm{i}(\lambda\sigma_3 + Q),\\ V(x,t;\lambda) &\equiv \mathrm{i}(\lambda^2\sigma_3 + \lambda Q) - \tfrac{1}{2}\sigma_3(\mathrm{i}Q^2 - Q_x), \end{aligned}$$

and

$$\sigma_3 = \mathrm{diag}(1,1,-1,-1),\ Q = \begin{bmatrix} \mathbf{0} & \sigma\mathbf{q}^\dagger \\ \mathbf{q} & \mathbf{0} \end{bmatrix},\ \mathbf{q} = \begin{bmatrix} q_1 & q_2 \\ q_2 & q_1 \end{bmatrix}.$$

The compatibility condition for the Lax pair equations (2) $\Phi_{xt} = \Phi_{tx}$ yields the CNLS-p (1). Thus we can study nonlinear dynamics of CNLS-p with the aid of the linear system (1). To obtain some interesting exact solutions for system (1), it is essential to derive the corresponding DT.

Before presenting the DT, we discuss some symmetries for a system (1). It is evident that Eq. (1) possess the following scaling transformation: Galileo transformation, time and space displacement invariants, and phase invariants. We would like to use these symmetries to reduce the parameters for solutions.

The linear system (2) is a reduction for the 2×2 matrix NLS [30]. The DT for the AKNS system is well known from different authors [31–33]. But for the reduction system, we need to find an additional symmetry relation to remain invariant of the DT. To find this relation, we investigate the following symmetry relations for matrices $U(\lambda)$ and $V(\lambda)$: the first reality condition [33],

$$U^\dagger(\bar{\lambda}) = -\sigma U(\lambda), \quad V^\dagger(\bar{\lambda}) = -\sigma V(\lambda), \tag{3}$$

which is the classical $su(4)$-reality condition [33]; and the second reality condition is

$$\Sigma U(\lambda)\Sigma = U(\lambda), \quad \Sigma V(\lambda)\Sigma = V(\lambda), \tag{4}$$

where

$$\Sigma = \begin{bmatrix} \sigma_1 & \mathbf{0} \\ \mathbf{0} & \sigma_1 \end{bmatrix}, \quad \sigma_1 = \begin{bmatrix} 0 & 1 \\ 1 & 0 \end{bmatrix}.$$

The DT for matrix NLS is obtained in Ref. [33] with the loop group method:

$$T = I - \frac{P_1}{\lambda - \overline{\lambda_1}}, \quad P_1 = \Phi_1\left(\frac{\Phi_1^\dagger J\Phi_1}{\lambda_1 - \overline{\lambda_1}}\right)^{-1}\Phi_1^\dagger J, \tag{5}$$

where Φ_1 is a special matrix solution for linear system (2) with $\lambda = \lambda_1$, and $J = \mathrm{diag}(1,1,\sigma,\sigma)$; the column of matrix Φ_1 can be one or two. By the above transformation, we can convert $(U(\lambda), V(\lambda))$ of the system (2) into $(U[1](\lambda), V[1](\lambda))$, where

$$\begin{aligned} U[1](\lambda) &= T_x T^{-1} + TU(\lambda)T^{-1},\\ V[1](\lambda) &= T_t T^{-1} + TV(\lambda)T^{-1}. \end{aligned}$$

To keep the second reality condition for the new system $(U[1](\lambda), V[1](\lambda))$, we need to restrict the Darboux matrix $T(\lambda) = \Sigma T(\lambda)\Sigma$. We give two different reductions through the rank of P_1.

For the first case, the column of matrix solution Φ_1 is one. Furthermore, we have $\Phi_1\Phi_1^\dagger J = \Sigma\Phi_1\Phi_1^\dagger J\Sigma$, i.e., $\Phi_1 = \delta\Sigma\Phi_1$, $\delta = \pm 1$. This kind of DT was derived in Ref. [16]. It is evident that the DT is constructed through a special vector solution possessing special symmetry. A natural problem is how to use the other vector solution to construct the DT. To complete this aim, we give another type of reduction.

For the second case, the column of the matrix solution Φ_1 is two. Furthermore we have $\Phi_1(\Phi_1^\dagger J\Phi_1)^{-1}\Phi_1^\dagger J = \Sigma\Phi_1(\Phi_1^\dagger J\Phi_1)^{-1}\Phi_1^\dagger J\Sigma$, where $\Phi_1 = [\Psi_1, \widehat{\Psi}_1]$, Ψ_1 and $\widehat{\Psi}_1$ are two linear independent vector solutions for the linear system (2) at $\lambda = \lambda_1$. To keep the linear system with the symmetry relation, we choose $\widehat{\Psi}_1 = \delta\Sigma\Psi_1$. If Ψ_1 is a special vector solution without the symmetry $\Psi_1 = \delta\Sigma\Psi_1$ for the linear system at $\lambda = \lambda_1$, then $\delta\Sigma\Psi_1$ is also a special vector solution by the symmetry relation (4). It follows that we can use this solution to construct the DT. We can see that the second case is a supplement for the first case.

In what follows, we use the special vector solution Ω_1 to construct the Darboux matrix and exact solution for Eq. (1). In the first case, when $\Omega_1 = \delta\Sigma\Omega_1$, then set $|y_1\rangle = A(x,t)\Omega_1$, $A(x,t)$ is the appropriate nonsingular function to simplify the calculation, and the DT is

$$\begin{aligned} T_1 &= I - \frac{\lambda_1 - \overline{\lambda_1}}{\lambda - \overline{\lambda_1}}\frac{|y_1\rangle\langle y_1|J}{\langle y_1|J|y_1\rangle},\\ |y_1\rangle &= [\phi_1, \quad \delta\phi_1, \quad \delta\psi_1, \quad \psi_1]^T, \quad \langle y_1| = |y_1\rangle^\dagger, \end{aligned} \tag{6}$$

and the transformations between the q_1, q_2, and $q_1[1]$, $q_2[1]$ are

$$q_1[1] = q_1 - \frac{\delta\psi_1\bar{\phi}_1}{(|\phi_1|^2 + \sigma|\psi_1|^2)/(\lambda_1 - \overline{\lambda_1})},$$
$$q_2[1] = q_2 - \frac{\psi_1\bar{\phi}_1}{(|\phi_1|^2 + \sigma|\psi_1|^2)/(\lambda_1 - \overline{\lambda_1})}. \tag{7}$$

When $\Omega_1 \neq \delta\Sigma\Omega_1$, $\Phi_1 = A(x,t)[\Omega_1, \delta\Sigma\Omega_1]$, we can construct the second form for Darboux matrix:

$$T_2 = I - \frac{\lambda_1 - \overline{\lambda_1}}{\lambda - \overline{\lambda_1}}\Phi_1(\Phi_1^\dagger J \Phi_1)^{-1}\Phi_1^\dagger J,$$
$$\Phi_1 = \begin{bmatrix} \phi_1 & \varphi_1 & \chi_1 & \psi_1 \\ \delta\varphi_1 & \delta\phi_1 & \delta\psi_1 & \delta\chi_1 \end{bmatrix}^T, \tag{8}$$

and the transformations between the q_1, q_2 and $q_1[1]$, $q_2[1]$ are

$$q_1[1] = q_1 - N_1 - N_2, \quad q_2[1] = q_2 + N_1 - N_2, \tag{9}$$

where

$$N_1 = \frac{(\bar{\varphi}_1 - \bar{\phi}_1)(\psi_1 - \chi_1)}{(|\varphi_1 - \phi_1|^2 + \sigma|\psi_1 - \chi_1|^2)/(\lambda_1 - \overline{\lambda_1})},$$
$$N_2 = \frac{(\bar{\varphi}_1 + \bar{\phi}_1)(\psi_1 + \chi_1)}{(|\varphi_1 + \phi_1|^2 + \sigma|\psi_1 + \chi_1|^2)/(\lambda_1 - \overline{\lambda_1})}.$$

The above formulas (7) and (9) could be nonsingular with the limit $\lambda_1 \to \overline{\lambda_1}$ for the defocusing case, which can be used to construct the dark-type soliton solution [34]. Performing the transformation, we can derive different kinds of nonlinear wave solutions from related seed solutions.

The two forms for DT presented above can be used to construct single and double nonlinear localized waves separately. For the attractive case, we find that kink-like breather, the rogue wave with particle transition, can exist in the two-component coupled system. For the repulsive case, the stable kink-dark soliton can exist in the coupled system. Their dynamics are all different from the ones reported before [16–19]. In particular, we present the localized wave pair as linear superpositions of well-known solutions of simplest NLSE. In the follows, we list all nontrivial solutions for the system (1) in two cases according to the two DT forms.

IV. SOLUTIONS DERIVED FROM THE FIRST DT FORM

The solution obtained through the first kind of DT can be represented as follows:

$$q_1[1] = \left[\frac{1}{2} + \frac{v e^{-2i\theta}}{2}\right]e^{i\sigma t}, \quad q_2[1] = \left[\frac{1}{2} - \frac{v e^{-2i\theta}}{2}\right]e^{i\sigma t}, \tag{10}$$

where $\theta \in [0,\pi/2]$. The first term of the solution in each component denotes a plane wave background, which means that the localized waves are excited in a Bose-Einstein condensate with homogeneous particle density. There are two cases for the coupled system: attractive and repulsive interactions between atoms. The system admits different nonlinear excitations for the two cases. For different localized waves, the expressions of v are different in the above solution. We discuss them separately as follows.

A. Attractive case $\sigma = 1$

There are three main types of nonlinear localized waves: breather with periodic particle transition, kink-type (waterfall type) breathe, and rogue wave (beak type). We present them one by one as follows.

1. Breather with periodic particle transition

Choosing $v = S(\alpha_1,\beta_1;a_1,b_1)e^{i(2\theta - t)}$ where

$$S(\alpha_1,\beta_1;a_1,b_1) = \frac{2i\beta_1 e^{-2i[\alpha_1 x + (\alpha_1^2 - \beta_1^2)t] + ib_1}}{\cosh[2\beta_1(x + 2\alpha_1 t) + a_1]}, \tag{11}$$

and a_1, b_1 are real parameters, we can obtain a breather on the plane wave background along the line $2\beta_1(x + 2\alpha_1 t) + a_1 = 0$, which oscillates with the line vertical to $2[\alpha_1 x + (\alpha_1^2 - \beta_1^2)t] - b_1 - \pi/2 = 0$ with period 2π. Particle transition emerges periodically with time. Moreover, we find that the oscillation is not a standard cosine or sine type as in standard Josephson oscillation [35]. Instead, it has been modified by the nonlinear interactions, similar to the nonlinear Josephson effects observed in BEC experiments [36].

2. Kink-type breather solution

Setting $v = B(x_1,t_1)$, where

$$B(x_1,t_1) \equiv \frac{\cosh(\kappa_1)\cosh(A_1 + 2i\vartheta_1) + \sin(\vartheta_1)\cos(A_2 + 2i\kappa_1)}{\cosh(\kappa_1)\cosh(A_1) - \sin(\vartheta_1)\cos(A_2)} \tag{12}$$

and

$$A_1 = 2\sin(\vartheta_1)[\sinh(\kappa_1)(x - x_1) + \cos(\vartheta_1)(2\cosh^2(\kappa_1) - 1)(t - t_1)],$$
$$A_2 = 2\cosh(\kappa_1)[\cos(\vartheta_1)(x - x_1) + \sinh(\kappa_1)(2\cos^2(\vartheta_1) - 1)(t - t_1)].$$

x_1 and t_1 are real constants; they determine the localized wave's location on the temporal-spatial distribution plane. This is a kink-type breather, as shown in Fig. 1. The periodic humps located along the spatial dimension at a certain time, which are very similar to the Akhmediev breather in NLS or CNLS without particle transition. But the background amplitudes before and after the periodic humps emerging are quite different, namely, a large amount of particles' transition happen near the certain time, and they do not transit back. This can be proved precisely by the asymptotical analysis. The striking transition behavior is quite different from the related transition process or tunneling process studied in Refs. [9–11]. The whole particles are kept well since the whole Hamiltonian is a Hermitian operator. This can be proven by calculating the particle number in one whole period.

3. Rogue wave solution

Let $v = -R(x_1,t_1)$, where

$$R(x_1,t_1) \equiv 1 - \frac{4[2i(t - t_1) + 1]}{1 + 4(x - x_1)^2 + 4(t - t_1)^2}; \tag{13}$$

we can obtain a beak-type rogue wave solution, shown in Fig. 2. For the rogue wave in $|q_1|^2$, there are one hump

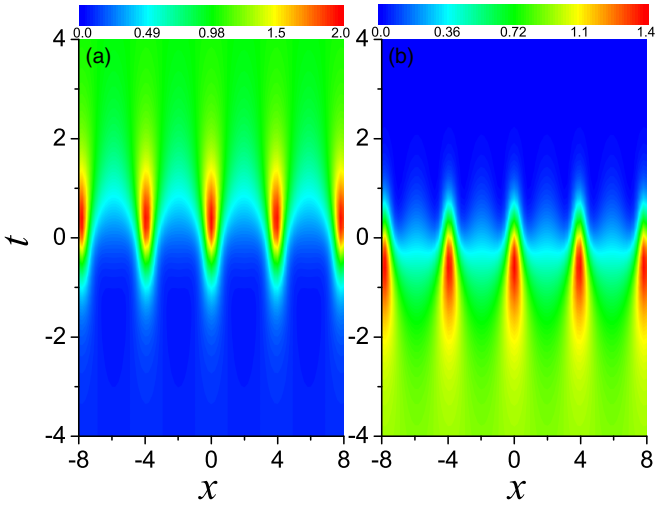

FIG. 1. (Color online) The dynamics of waterfall structure nonlinear waves: (a) for component q_1 and (b) for component q_2. It is seen that the background amplitudes before and after the breather emerges are unequal, in contrast to the breather reported before. This corresponds to a drastic nonlinear particle transition behavior. Parameters: $\theta = \arccos(\frac{4}{5})$, $\vartheta_1 = \arcsin(\frac{3}{5})$, and $\kappa_1 = 0$.

and two valleys on the temporal-spatial distribution, which admits a distinctive spatial-temporal distribution, in contrast to the well-known eye-shaped structure, four-petaled flower structure, and anti-eye-shaped structure [37]. The structure of the rogue wave is inverse for the $|q_2|^2$. Also the particle number is not conserved for each component. Different from the kink type breather, the particles transit back. This kind of structure is not observed in other integrable models [7,8,37–39]. The hump in one component corresponds to two valleys in the other component, which clearly demonstrate the transition dynamics between the two components. The one hump and two valleys structure for a fundamental rogue wave can be proven

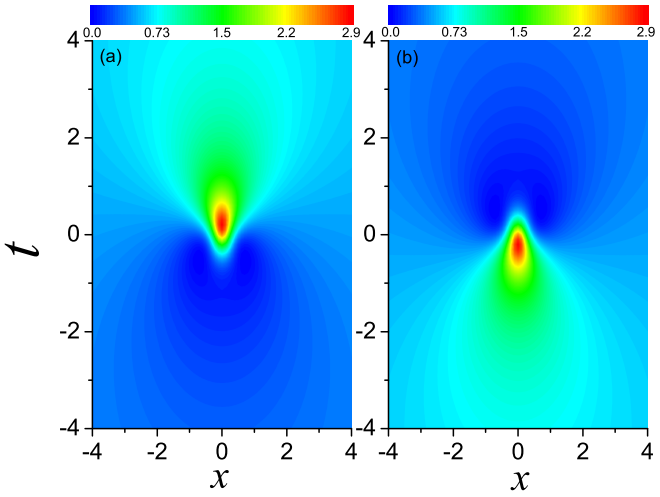

FIG. 2. (Color online) Fundamental rogue wave which possesses one hump and two valleys: (a) for component q_1 and (b) for component q_2. It is seen that the pattern is quite different from the eye-shaped rogue wave reported before. Parameters: $\theta = \arccos(\frac{\sqrt{2}}{2})$, $x_1 = t_1 = 0$.

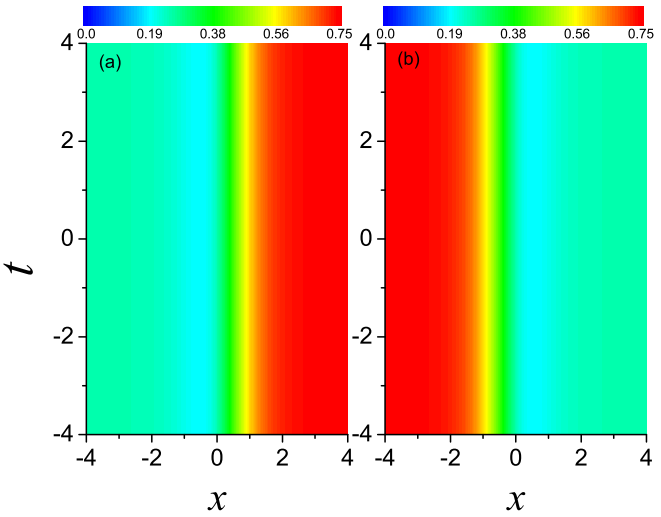

FIG. 3. (Color online) The evolution of kink-dark waves: (a) for component q_1 and (b) for component q_2. It is seen that there are a kink and a dark soliton coexisting in the intensity distribution. Parameters: $c_1 = 0$, $\theta = \pi/6$, $\vartheta_2 = \pi/2$.

exactly through calculating the extreme points. For different θ values, we can obtain different structures for the fundamental beak-type rogue wave. When $\theta = 0, \pi/2$, the structure can be reduced to the ones considered in Ref. [16].

B. Repulsive case $\sigma = -1$

In this case, we derive a kink solution, which has not been found in CNLS with no particle transition and in NLS with repulsive interactions.

1. Kink-dark soliton solution

We choose $v = D(c_1)$, where

$$D(c_1) = [\cos(\vartheta_2) + \mathrm{i}\sin(\vartheta_2)\tanh(Y_1)]\exp(-\mathrm{i}\vartheta_2) \tag{14}$$

and

$$Y_1 = \sin(\vartheta_2)[x + \cos(\vartheta_2)t + c_1];$$

c_1 is real constant, $0 < \vartheta_2 < \pi$. Then we can obtain the topological kink-dark soliton excitations. For example, we demonstrate one case for the kink-dark soliton in Fig. 3. With different values of θ and ϑ_2, one can obtain dark soliton and kink waves with many different structures independently. These kink-dark solitons are very stable against small perturbations, since there is no modulational instability in the system with repulsive interactions.

V. PAIR SOLUTIONS DERIVED FROM THE SECOND DT FORM

The solution obtained by the second DT could be represented as follows:

$$\begin{aligned} q_1[1] &= \left[\frac{v_1}{2} + \frac{v_2 \mathrm{e}^{-2\mathrm{i}\theta}}{2}\right]\mathrm{e}^{\mathrm{i}\sigma t}, \\ q_2[1] &= \left[\frac{v_1}{2} - \frac{v_2 \mathrm{e}^{-2\mathrm{i}\theta}}{2}\right]\mathrm{e}^{\mathrm{i}\sigma t}. \end{aligned} \tag{15}$$

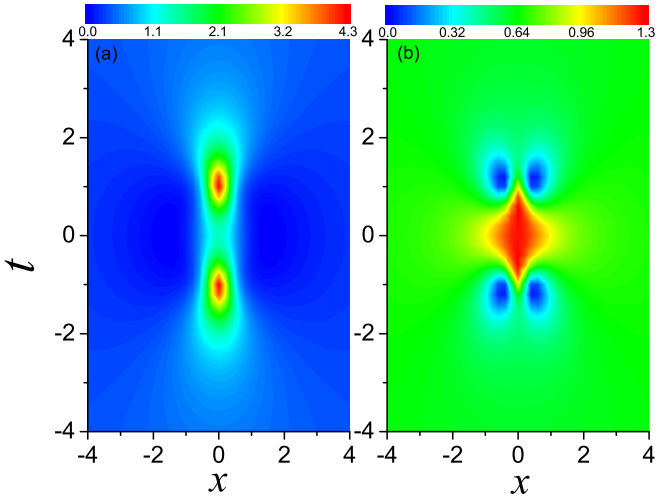

FIG. 4. (Color online) The evolution of rogue wave and rogue wave pair in the coupled model: (a) for component q_1 and (b) for component q_2. Parameters: $\theta = \arccos(3/5)$, $x_1 = 0$, and $t_1 = 1$.

This transformation form brings a localized wave pair to the coupled system. The localized wave pair solutions can be written as a linear superposition form of well-known solutions of the simplest NLS. This is a striking character for the coupled model with particle transition terms, in contrast to the CNLS without particle transition terms. The results are still presented as two cases according to interactions between atoms.

A. Attractive case $\sigma = 1$

There are mainly five types of nonlinear localized wave pairs as follows.

1. Breather and soliton pair

We choose $v_1 = B(x_1,t_1)$ and $v_2 = S(\sinh(\kappa_1)\cos(\vartheta_1), \cosh(\kappa_1)\sin(\vartheta_1); a_1,b_1)e^{i(2\theta-t)}$ where the expressions of B and S are given in (12) and (11), respectively. When the breather and soliton possesses different velocities, they behave like two breathers interacting. When breather and soliton possess the same velocity (it must be zero), they behave as a breather possessing a different oscillating behavior with a classical Ma breather.

2. Breather and rogue wave pair

We choose $v_1 = -R(x_1,t_1)$ and $v_2 = S(0,1;a_1,b_1)e^{i(2\theta-t)}$ where the expressions of R and S are given in (13) and (11), respectively. The breather is stationary and vibrates on the plane wave background, and the rogue wave is the fundamental rogue wave. The particle transition always happens near the locations of humps. Based on the solution, we can observe the interaction of a breather and rogue wave at many different cases conveniently though varying the parameters x_1, t_1, a_1, and b_1.

3. Breather and breather pair

We choose $v_1 = B(x_1,t_1)$ and $v_2 = B(-x_1,-t_1)$ where the expressions of B is given in (12). They behave as two breathers coexist with the same velocity. The periodic transition dynamics is kept well for the breather pair. This indicates that the transition period is determined by the initial breather condition.

4. Rogue wave and rogue wave pair

Choosing $v_1 = -R(x_1,t_1)$ and $v_2 = -R(-x_1,-t_1)$, we can obtain the rogue wave and rogue wave pair solution. When the distance between two rogue waves is far enough, they behave as two rogue waves' superposition on the plane wave background. When the distance of two rogue waves is close, their interaction will induce new behaviors. As an example, we demonstrate one case in Fig. 4. It is seen that there are two humps in one component, and correspondingly there are four valleys in the other component. There are also some complicated transition dynamics which come from the interaction between two rogue waves.

5. Soliton and soliton pair

We choose $v_1 = S(a_1,b_1)e^{-it}$ and $v_2 = S(-a_1,-b_1)e^{i(2\theta-t)}$, where the expressions of $S(a_1,b_1)$ and $S(-a_1,-b_1)$ are given in Eq. (11). From the expression, we can find the soliton solution is composed of a linear combination of two classical soliton solutions of the NLS with the same velocity. The shape of soliton will be appear as two cases: one is a bell shape, the other is an M shape. Similar properties are reported in Ref. [29] for the nonintegrable coupled NLS. However, this phenomenon never appears in classical NLSs or multicomponent integrable NLSs. This partly indicates that the pair-transition effects play a nontrivial role in the structure and dynamics of nonlinear excitations.

B. Repulsive case $\sigma = -1$

In this case, we only obtain the dark-dark soliton pair solution by the second DT form.

1. Kink-dark soliton pair

We choose $v_1 = D(c_1)$ and $v_2 = D(-c_1)$, where $D(c_1)$ and $D(-c_1)$ are given in Eq. (14). The linear combination of kink-dark and dark soliton solutions would demonstrate some novel stable excitation structures, e.g., W-shape, top hat-shape, and hole-shape. The explicit conditions for their existence can be analyzed precisely. This is meaningful for nonlinear localized wave applications.

The stability is very important to the solution in a nonlinear equation, and now we discuss this issue for these nonlinear excitations. We simulate the localized waves by numerical calculation from the initial condition given by the exact solution through performing the finite difference method [40,41]. It indicates that these nonlinear localized waves can be excited in the system even with some small noises. The kink-dark soliton and dark-dark soliton pair are very robust against perturbations since there is no modulational instability for the coupled model with repulsive interactions. And the soliton and soliton pair are also robust against perturbations. The breather and rogue wave can be evolved from corresponding initial conditions with small noises. But there are some other localized waves emerging after long time evolution, induced by the modulational instability of the background fields [42].

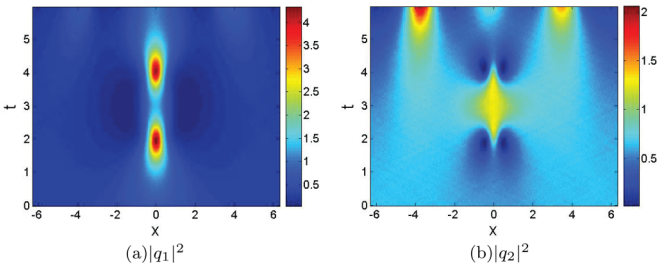

FIG. 5. (Color online) The numerical simulation of the rogue wave and rogue wave pair with small noise. The initial excitation condition is given by the exact ones at $t = -3$ in Fig. 4 by multiplying a factor $(1 + 0.01\,Random[-1,1])$. It is seen that the rogue wave pair are robust against small noise.

For instance, we show the simulation results for the rogue wave and rogue wave pair in Fig. 5, for which we use the initial excitation form given by the exact ones at $t = -3$ in Fig. 4 with adding small noise [by multiplying a factor $(1 + 0.01\,Random[-1,1])$]. It is seen that their is are similar during the first five scalar units from the same initial excitation. Some other localized waves emerge after the rogue wave pair emerging, which comes from the modulational instability [43]. This partly means that the localized wave obtained here can be excited in a real condensate system. It should be mentioned that some more rigorous or analytical stability results exist for rogue wave and breather solutions to NLSs [44–46].

VI. POSSIBILITIES TO OBSERVE THESE NONLINEAR EXCITATIONS

Recently, rogue waves and Akhmediev breathers have been excited experimentally in a nonlinear fiber system under the direction of related exact solutions [47,48]. Vector solitons including dark-dark, bright-dark solitons, bright-bright solitons, and even half-solitons have been excited experimentally in a multicomponent Bose-Einstein condensate based on density and phase modulation techniques [49]. The experiments indicated that the initial conditions for these nonlinear excitations can be made nearly precisely by density and phase modulation techniques. The pair-transition (PT) term corresponds to pair particle transition in a two-component Bose-Einstein condensate [20,21] or four-wave-mixing effect in a nonlinear planar waveguide [27,28]. The nonlinear localized waves obtained here are all superposed by the well-known nonlinear excitations which have been realized in real experiments. Moreover, the numerical simulations indicate that these nonlinear localized waves are robust against small perturbations or noises. Therefore, they can be realized in a two-component ultracold atomic system or planar waveguide with two orthogonal modes through combining these intensity and phase modulation techniques. As an example, we discuss possibilities to observe the rogue wave and rogue wave pair as shown in Fig. 4 in a cigar-shaped condensate with two hyperfine states, q_1 and q_2.

For simplicity, we assume the initial condensation occurring in the trapped state q_2. State q_1 is coupled to q_2 by an RF or microwave field tuned near the $q_2 \to q_1$ transition. The PT effects can be realized by the RF field in the strong interaction regimes [22,23]. The total number of ^{87}Rb atoms in the condensate is $N = 5 \times 10^4$. $a_{i,j}(i,j = 1,2)$ are s-wave scattering lengths which can be adjusted by Feshbach resonance technique. Setting $a_{1,2} = a_{2,1} = 1.6$ nm and $a_{2,2} = a_{1,1} = 0.8$ nm, under mean-field approximation, the s-wave scattering effective interaction strengths between atoms in the same hyperfine state are $U_{j,j} = 4\pi\hbar^2 a_{j,j}/m$ (m is the atom mass), and the scattering effective interaction strengths between atoms in different hyperfine state are $U_{j,3-j} = 4\pi\hbar^2 a_{j,3-j}/m$. When the interaction between atoms is attractive and the PT coefficient is $NU_{1,1}$, the units in the axial direction and time are scaled to be 2.0 μm and 0.5 ms, respectively, and the dynamics of the condensate with PT effects can be described well by Eq. (1). The exact solution (15) for the rogue wave and rogue wave pair with $\theta = \arccos(3/5)$, $x_1 = 0$, and $t_1 = 1$ can be used to direct initial density and phase modulation explicitly in the two components. It has been shown that the density and phase of Bose condensate can be manipulated nearly precisely [3]. The time of the transition process is about 2.5 ms for the rogue wave and rogue wave pair. The time duration is much shorter than the life time of a Bose condensate. The localized size of the rogue wave pair is about 12.0 μm on the spatial distribution, which means the plane wave background can be approached well by a much wider envelope. Moreover, the above numerical simulation has shown that the evolution of these nonlinear excitations is robust against small noises or perturbations. Therefore, the localized waves can be observed from the initial conditions approaching the ideal ones given by these exact solutions in the two-component condensate system.

VII. CONCLUSION AND DISCUSSION

In conclusion, we present two different DT forms for the CNLS-p with attractive or repulsive interactions, which can be used to describe transition dynamics of a one-dimensional two-component Bose-Einstein condensate system with particle transition in strong interaction regimes and other nonlinear systems [24–28]. Based on exact solutions of the coupled model, we predict that some new dynamics of nonlinear excitations can exist, such as the striking transition dynamics of breather, new excitation patterns for rogue waves, topological kink excitations, and other new stable excitation structures. The solution can be written as a linear superposition of nonlinear wave solutions of the simplest scalar NLS. Possibilities to observe them are discussed in a cigar-shaped condensate with two hyperfine states. The results here can be extended to other multicomponent NLSs or matrix NLS system, which creates opportunities to study the tunneling or transition dynamics of nonlinear localized waves exactly and analytically.

ACKNOWLEDGMENTS

This work is supported by National Natural Science Foundation of China (Contacts No. 11401221 and No. 11405129) and Fundamental Research Funds for the Central Universities (Contact No. 2014ZB0034).

[1] M. J. Ablowitz and Z. H. Musslimani, Phys. Rev. Lett. **110**, 064105 (2013).

[2] M. Onorato, S. Residori, U. Bortolozzo, A. Montina, and F. T. Arecchi, Phys. Rep. **528**, 47 (2013).

[3] P. G. Kevrekidis, D. Frantzeskakis, and R. Carretero-Gonzalez, *Emergent Nonlinear Phenomena in Bose-Einstein Condensates: Theory and Experiment* (Springer, Berlin, 2009).

[4] C. Becker, S. Stellmer, P. S. Panahi, S. Dorscher, M. Baumert, Eva-Maria Richter, J. Kronjager, K. Bongs, and K. Sengstock, Nature Phys. **4**, 496 (2008).

[5] Y. V. Bludov, V. V. Konotop, and N. Akhmediev, Eur. Phys. J. Special Topics **185**, 169 (2010).

[6] T. Kanna and M. Lakshmanan, Phys. Rev. Lett. **86**, 5043 (2001); M. Vijayajayanthi, T. Kanna, and M. Lakshmanan, Phys. Rev. A **77**, 013820 (2008).

[7] F. Baronio, A. Degasperis, M. Conforti, and S. Wabnitz, Phys. Rev. Lett. **109**, 044102 (2012).

[8] L. C. Zhao and J. Liu, J. Opt. Soc. Am. B **29**, 3119 (2012).

[9] J. Williams, R. Walser, J. Cooper, E. Cornell, and M. Holland, Phys. Rev. A **59**, R31(R) (1999); J. Williams, R. Walser, J. Cooper, E. A. Cornell, and M. Holland, *ibid.* **61**, 033612 (2000).

[10] U. R. Fischer, C. Iniotakis, and A. Posazhennikova, Phys. Rev. A **77**, 031602(R) (2008).

[11] J. Liu, L. Fu, B.-Y. Ou, S.-G. Chen, Dae-Il Choi, B. Wu, and Q. Niu, Phys. Rev. A **66**, 023404 (2002).

[12] J. Ieda, T. Miyakawa, and M. Wadati, Phys. Rev. Lett. **93**, 194102 (2004).

[13] Z. J. Qin and G. Mu, Phys. Rev. E **86**, 036601 (2012).

[14] Y. Lahini, F. Pozzi, M. Sorel, R. Morandotti, D. N. Christodoulides, and Y. Silberberg, Phys. Rev. Lett. **101**, 193901 (2008).

[15] Y. Y. Li, W. Pang, S. H. Fu, and B. A. Malomed, Phys. Rev. A **85**, 053821 (2012).

[16] L. C. Zhao, L. Ling, Z. Y. Yang, and J. Liu, Commun. Nonlinear Sci. Numer. Simulat. **23**, 21 (2015).

[17] Q.-H. Park and H. J. Shin, Phys. Rev. E **59**, 2373 (1999).

[18] X. Lü and B. Tian, Phys. Rev. E **85**, 026117 (2012).

[19] W. R. Sun, B. Tian, Y. Jiang, and H. L. Zhen, Phys. Rev. E **91**, 023205 (2015).

[20] P. Bader and U. R. Fischer, Phys. Rev. Lett. **103**, 060402 (2009).

[21] U. R. Fischer, K. S. Lee, and B. Xiong, Phys. Rev. A **84**, 011604 (2011).

[22] S. Fölling, S. Trotzky, P. Cheinet, M. Feld, R. Saers, A. Widera, T. Müller, and I. Bloch, Nature (London) **448**, 1029 (2007).

[23] S. Zöllner, H. D. Meyer, and P. Schmelcher, Phys. Rev. Lett. **100**, 040401 (2008).

[24] Boris A. Malomed, Phys. Rev. A **45**, R8321 (1992).

[25] D. Y. Tang, B. Zhao, D. Y. Shen, C. Lu, W. S. Man, and H. Y. Tam, Phys. Rev. A **66**, 033806 (2002).

[26] W. J. Liu, N. Pan, L. G. Huang, and M. Lei, Nonlinear Dyn. **78**, 755 (2014).

[27] C. R. Menyuk, IEEE J. Quantum Electron. **QE-23**, 174 (1987).

[28] J. U. Kang, G. I. Stegeman, J. S. Aitchison, and N. Akhmediev, Phys. Rev. Lett. **76**, 3699 (1996).

[29] J. Yang and D. J. Benney, Stud. Appl. Math. **96**, 111 (1996).

[30] A. P. Fordy and P. P. Kulish, Commun. Math. Phys. **89**, 427 (1983).

[31] V. B. Matveev and M. A. Salle, *DTs and Solitons* (Springer, Berlin, 1991).

[32] C. H. Gu, H. S. Hu, and Z. Zhou, *DTs in Integrable Systems: Theory and Their Applications to Geometry* (Springer, Dordrecht, 2006).

[33] C. L. Terng and K. Uhlenbeck, Comm. Pure Appl. Math. **53**, 1 (2000).

[34] L. Ling, L. C. Zhao, and B. Guo, arXiv:1407.5194.

[35] B. D. Josephson, Phys. Lett. **1**, 251 (1962).

[36] M. Albiez, R. Gati, J. Fölling, S. Hunsmann, M. Cristiani, and M. K. Oberthaler, Phys. Rev. Lett. **95**, 010402 (2005).

[37] L. C. Zhao, G. G. Xin, and Z. Y. Yang, Phys. Rev. E **90**, 022918 (2014).

[38] B. L. Guo and L. M. Ling, Chin. Phys. Lett. **28**, 110202 (2011).

[39] F. Baronio, M. Conforti, A. Degasperis, S. Lombardo, M. Onorato, and S. Wabnitz, Phys. Rev. Lett. **113**, 034101 (2014).

[40] L. Lee, G. Lyng, and I. Vankova, Physica D **241**, 1767 (2012).

[41] W. Z. Bao, Q. L. Tang, and Z. G. Xu, J. Comput. Phys. **235**, 423 (2013).

[42] S. H. Chen, P. Grelu, and J. M. Soto-Crespo, Phys. Rev. E **89**, 011201(R) (2014).

[43] S. H. Chen, J. M. Soto-Crespo, and P. Grelu, Opt. Express **23**, 349 (2015).

[44] A. Ankiewicz, N. Devine, and N. Akhmediev, Phys. Lett. A **373**, 3997 (2009).

[45] Robert A. Van Gorder, J. Phys. Soc. Jpn. **83**, 054005 (2014).

[46] V. E. Zakharov and A. A. Gelash, Phys. Rev. Lett. **111**, 054101 (2013).

[47] J. M. Dudley, G. Genty, F. Dias, B. Kibler, and N. Akhmediev, Opt. Express **17**, 21497 (2009).

[48] B. Kibler, J. Fatome, C. Finot, G. Millot *et al.*, Nature Phys. **6**, 790 (2010); Sci. Rep. **2**, 463 (2012).

[49] C. Hamner, J. J. Chang, P. Engels, and M. A. Hoefer, Phys. Rev. Lett. **106**, 065302 (2011); M. A. Hoefer, J. J. Chang, C. Hamner, and P. Engels, Phys. Rev. A **84**, 041605(R) (2011).